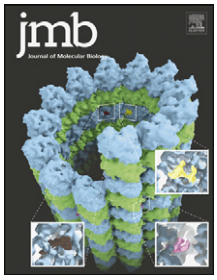

Insights into the Distinct Mechanisms of Action of Taxane and Non-Taxane Microtubule Stabilizers from Cryo-EM Structures

Elizabeth H. Kellogg [1], Nisreen M.A. Hejab [2], Stuart Howes [3,8], Peter Northcote [4], John H. Miller [4], J. Fernando Díaz [5], Kenneth H. Downing [1] and Eva Nogales [1,6,7]

*1 - **Molecular Biophysics and Integrated Bioimaging Division,** Lawrence Berkeley National Laboratory, Berkeley, CA 94720, USA*
*2 - **Graduate Group in Comparative Biochemistry,** UC Berkeley, CA 94720, USA*
*3 - **Biophysics Graduate Group,** University of California, Berkeley, CA 94720, USA*
*4 - **Centre for Biodiscovery,** Victoria University of Wellington, 6140, Wellington, New Zealand*
*5 - **Chemical and Physical Biology,** Centro de Investigaciones Biológicas, Consejo Superior de Investigaciones Científicas, 28040 Madrid, Spain*
*6 - **QB3 Institute and Molecular and Cell Biology Department,** University of California, Berkeley, CA 94720-3220, USA*
*7 - **Howard Hughes Medical Institute,** University of California, Berkeley, CA 94720-3220, USA*

***Correspondence to Eva Nogales:** QB3 Institute and Molecular and Cell Biology Department, University of California, Berkeley, CA 94720-3220, USA. enogales@lbl.gov*
http://dx.doi.org/10.1016/j.jmb.2017.01.001
Edited by Thomas J. Smith

Abstract

A number of microtubule (MT)-stabilizing agents (MSAs) have demonstrated or predicted potential as anticancer agents, but a detailed structural basis for their mechanism of action is still lacking. We have obtained high-resolution (3.9–4.2 Å) cryo-electron microscopy (cryo-EM) reconstructions of MTs stabilized by the taxane-site binders Taxol and zampanolide, and by peloruside, which targets a distinct, non-taxoid pocket on β-tubulin. We find that each molecule has unique distinct structural effects on the MT lattice structure. Peloruside acts primarily at lateral contacts and has an effect on the "seam" of heterologous interactions, enforcing a conformation more similar to that of homologous (i.e., non-seam) contacts by which it regularizes the MT lattice. In contrast, binding of either Taxol or zampanolide induces MT heterogeneity. In doubly bound MTs, peloruside overrides the heterogeneity induced by Taxol binding. Our structural analysis illustrates distinct mechanisms of these drugs for stabilizing the MT lattice and is of relevance to the possible use of combinations of MSAs to regulate MT activity and improve therapeutic potential.
© 2017 The Authors. Published by Elsevier Ltd. This is an open access article under the CC BY-NC-ND license (http://creativecommons.org/licenses/by-nc-nd/4.0/).

Introduction

Microtubules (MTs) are crucial components of the cytoskeleton and play a central role in cell division. MTs are made of αβ-tubulin that assembles longitudinally into protofilaments (PFs). About 13 PFs are associated laterally, making the MT wall. Essential to MT function is the property of dynamic instability, the stochastic switching between MT growing and shrinking linked to GTP binding and hydrolysis [1]. MT dynamics are tightly regulated *in vivo* by a number of MT-associated proteins (MAPs) [2,3]. Widely successful antimitotic chemotherapeutics, such as Taxol, bind to and stabilize MTs, inhibiting dynamic instability and preventing cells from dividing [4,5]. Taxol and other stabilizing compounds also interfere with interphase MTs [6], thus affecting many essential cellular processes. Since its discovery [7], Taxol has been the subject of many studies aimed at identifying its mechanism of action [8].

Taxol binds to a pocket in β-tubulin [9] that faces the MT lumen and is near the lateral interface between PFs [9–11] (Fig. 1). This lateral interface is inherently flexible, as *in vitro* MTs can have different numbers of PFs, ranging typically from 12 to 15 [12,13]. A hinge-like mechanism, involving the "M-loop", appears to accommodate the variation in MT diameter with little change in the tubulin structure

0022-2836/© 2017 The Authors. Published by Elsevier Ltd. This is an open access article under the CC BY-NC-ND license (http://creativecommons.org/licenses/by-nc-nd/4.0/).

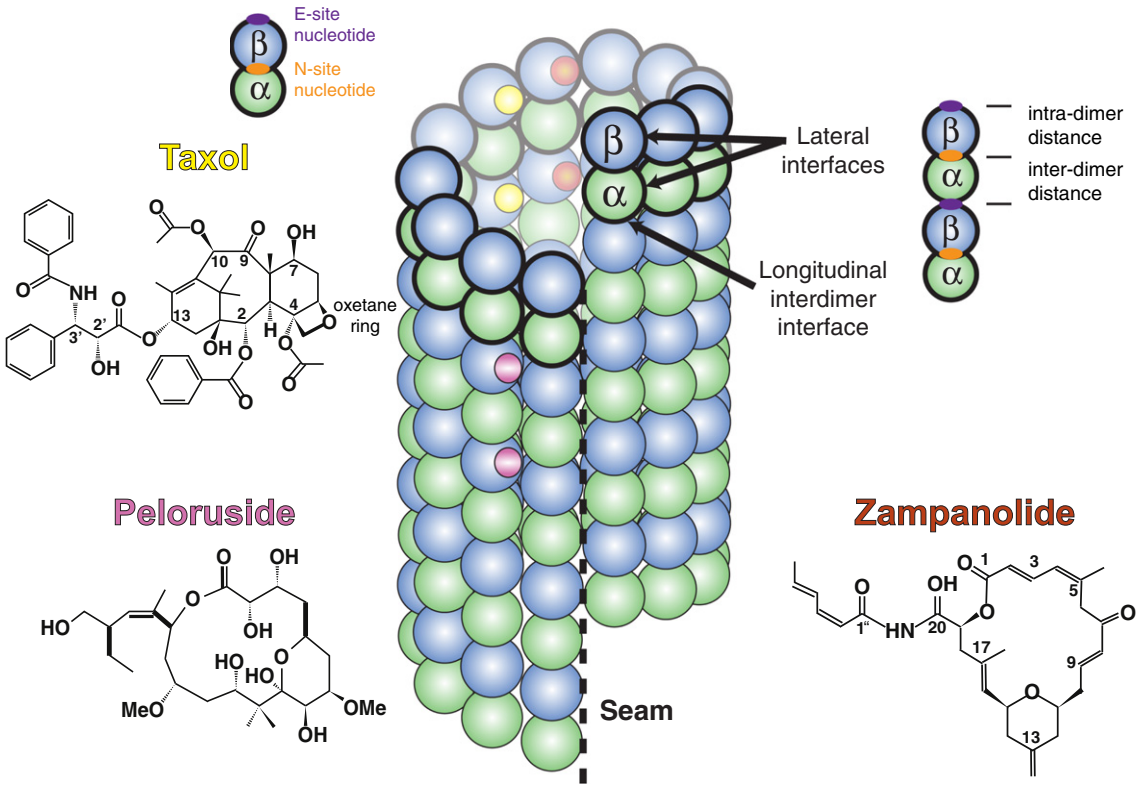

Fig. 1. Schematic of an MT and the binding sites for three MSAs. Taxol and zampanolide bind to the same lumenal binding pocket, whereas peloruside binds to a pocket located on the MT exterior. A schematic for the dimer shows the position of the N- and E-site nucleotides. The schematic for two dimers shows the distances between nucleotides that we refer to in the text as intra- and interdimer. The molecular structure for the three drugs used in this study is also shown.

[14]. While MTs formed *in vitro* have predominantly 13 and 14 PFs in the absence of binding factors or tubulin-targeting drugs, in the presence of Taxol, the distribution shifts to mostly 12 and 13 PFs [15,16], suggesting that Taxol has an effect on the lateral interface. On the other hand, Taxol has been shown to straighten individual PFs [17], suggesting an effect at the longitudinal interface between tubulin subunits. More recently, high-resolution cryo-electron microscopy (cryo-EM) studies comparing MTs in different nucleotide states have indicated that GTP hydrolysis leads to a compaction at the longitudinal interdimer interface, adjacent to the nucleotide in β-tubulin [11,18]. Interestingly, Taxol seems to reverse, at least partially, the effect of GTP hydrolysis, giving rise to a more expanded lattice after GTP hydrolysis [11,15,18]. Because the resolution in previous studies with Taxol [11] was limited to 5.5 Å, it was not possible to describe the details of this Taxol-induced lattice expansion, and the allosteric mechanism that links the Taxol-binding pocket to the longitudinal interfaces remains unknown.

Numerous cancer research efforts have been directed toward finding other natural small molecules that exert stabilizing effects similar to those of Taxol or toward synthesizing Taxol-like analogs. As a result, a growing number of taxane and non-taxane MT-stabilizing agents (MSAs) have been identified. Today, there is a plethora of structurally diverse MSAs, including epothilone [19], zampanolide [20], peloruside [21], discodermolide [22], and laulimalide [23], among others. In some cases, their binding site on tubulin has been described in atomic detail [24,25] in X-ray crystal structures of unassembled tubulin that, however, lacked information concerning the effect of these agents on the assembled MT structure. Many of these agents (such as epothilone and zampanolide) target the Taxol-binding pocket on the MT lumen and are generally known as taxane-site binders. Zampanolide is also known to form a covalent bond at the taxoid site [26]. Peloruside and laulimalide recognize a pocket on the surface of tubulin that faces the MT exterior [25]. The overall effects of peloruside and laulimalide are, however, similar to those of Taxol-site MSAs: MTs assemble more efficiently in their presence [27], and they inhibit MT dynamic instability [28] and cell division [29]. It has been described that the combined effect of a Taxol-site MSA (Taxol) with a peloruside-site MSA (referred to as doubly bound) results in a synergistic promotion of MT assembly and stabilization [30,31]. On the other hand, mechanical properties of the MT lattice appear

to be governed by one drug over the other [32], suggesting that the structural effects of a particular drug may dominate.

In spite of progress over the years, a complete understanding of the stabilizing mechanism of MSAs remains elusive. Knowledge of how Taxol and other small molecules affect MT structure would not only contribute to our understanding of MT dynamic instability but also provide crucial guidance to improve MSA design in efforts toward cancer treatment. Previous crystallographic studies have focused on the contribution of MSAs to the stabilization of the M-loop in β-tubulin, proposing as a mode of action the facilitation of lateral contacts between PFs [24,25]. Consistent with this idea, changes outside the drug-binding pocket are minimal in those crystal structures, suggesting that drugs either do not impact the global conformation of tubulin or, alternatively, that crystallization conditions or crystal packing overrides the effects of the drug. If the latter were the case, then the effects of the drug on tubulin structure could be more extensive in an MT lattice context, as it has proven to be the case concerning the state of the exchangeable (E-site) nucleotide in tubulin [11,18].

To characterize any such structural effects on the MT lattice and gain further insight into the mechanism of action of MT stabilizers, we have produced near-atomic resolution (3.9–4.2 Å) cryo-EM maps of MTs bound to three structurally diverse MSAs. We find that peloruside and the taxane-site binders Taxol and zampanolide have very different effects on MT lattice structure, suggesting distinct stabilizing mechanisms. Peloruside acts as a "wedge", affecting lateral contacts, most prominently at the seam. Taxol and zampanolide, which bind to the same site on tubulin, produce distinct lattice structures, and both give rise to structural heterogeneity in the MT walls. Finally, we find that peloruside in the doubly bound structure overrides the heterogeneity induced by Taxol in the doubly bound structure. In all three cases, the drug-induced changes in the structure of the tubulin dimer are small but produce significant and distinctive changes in the MT lattice.

Results

When differences between α- and β-tubulin are ignored, the arrangement of tubulin subunits in the MT follows a helical path, most commonly a three-start helix as depicted in Fig. 1. However, when the differences between α- and β-tubulin are taken into account, this helical symmetry is broken at the "seam", a discontinuity in the lateral contacts where interactions are heterotypic (α-β and β-α), in contrast with the rest of homotypic contacts around the MT cylinder. Nonetheless, helical symmetry can be used to relate two tubulin subunits in adjacent PFs using two "lattice parameters", the rise (translation along the helical axis, parallel to the seam) and the twist (rotation around the helical axis). Additional parameters useful in the description of the MT lattice are the dimer rise, or "axial repeat", which is the distance between dimers along a PF, and the dimer twist or "MT supertwist", which describes the angle between PFs and the axis of the MT (0 supertwist means that the PFs run parallel to the MT axis).

We prepared cryo-EM samples, following previously described procedures [11,18], for MT preparations stabilized by three different MSAs: Taxol, peloruside, and zampanolide. Table S1 summarizes the results concerning MT lattice parameters for the different samples. Comparison with the previously described GTP-like and GDP (guanosine diphosphate)-state MTs [11,18] provides a particularly useful context for understanding the effects of the drugs.

Effect of different MSAs on MT lattice parameters

Previous studies reported that adding Taxol to unassembled tubulin or to preformed MTs resulted in different distances between tubulin subunits along the PF [15], suggesting that the structural effects of Taxol may be different depending on whether it is added before tubulin incorporation into the lattice, and thus before GTP hydrolysis, or after MT assembly, and thus into a preexisting GDP-bound state. To further explore this possibility, we prepared Taxol-stabilized MTs for cryo-EM analysis using previously described protocols [11] but varied the time when the drug was added (before, i.e., pre-hydrolysis, or after lattice formation, i.e., post-hydrolysis). Two independent reconstructions of each sample type have roughly equivalent resolution (4.0 Å pre-hydrolysis MTs; 3.9 Å post-hydrolysis MTs;Figs. S1–S2).

Consistent with previous reports [15], the lattice parameters of the Taxol-MT reconstructions depended on whether Taxol was added to preformed MTs (post-hydrolysis state) or unassembled tubulin (pre-hydrolysis state;Table S1). Although we have data for MTs ranging from 12 to 15 PFs, we focus here on 13 PFs, as they were the most abundant across all conditions. Using the dimer axial repeat as a basis for comparison, our prior work showed that drug-free GMPCPP-MTs (corresponding to a GTP-like state) have an "expanded lattice" with an 83.2 Å axial repeat, whereas dynamic, GDP-bound MTs have a "compacted lattice" with an axial repeat of 81.5 Å [11,18]. Taxol-MTs in which Taxol is added to preformed MTs have an axial repeat of 81.8 Å, very similar to that of the drug-free MT lattice. However, when added to unassembled tubulin, Taxol results in a noticeable lattice expansion, with an axial repeat of 82.3 Å (Table S1), consistent with a model in which Taxol inhibits, at least partially, the structural transition that occurs upon GTP hydrolysis. Although the measured axial repeat for the pre-hydrolysis Taxol sample is

smaller than previously reported [11], this state is consistently observed to be expanded with respect to the drug-free GDP-MT reconstruction, indicating that the structural changes, while subtle, are robust.

In contrast to Taxol, little is known about how other drugs, such as zampanolide or peloruside, affect the MT lattice. To investigate their effect, we performed similar experiments for both peloruside and

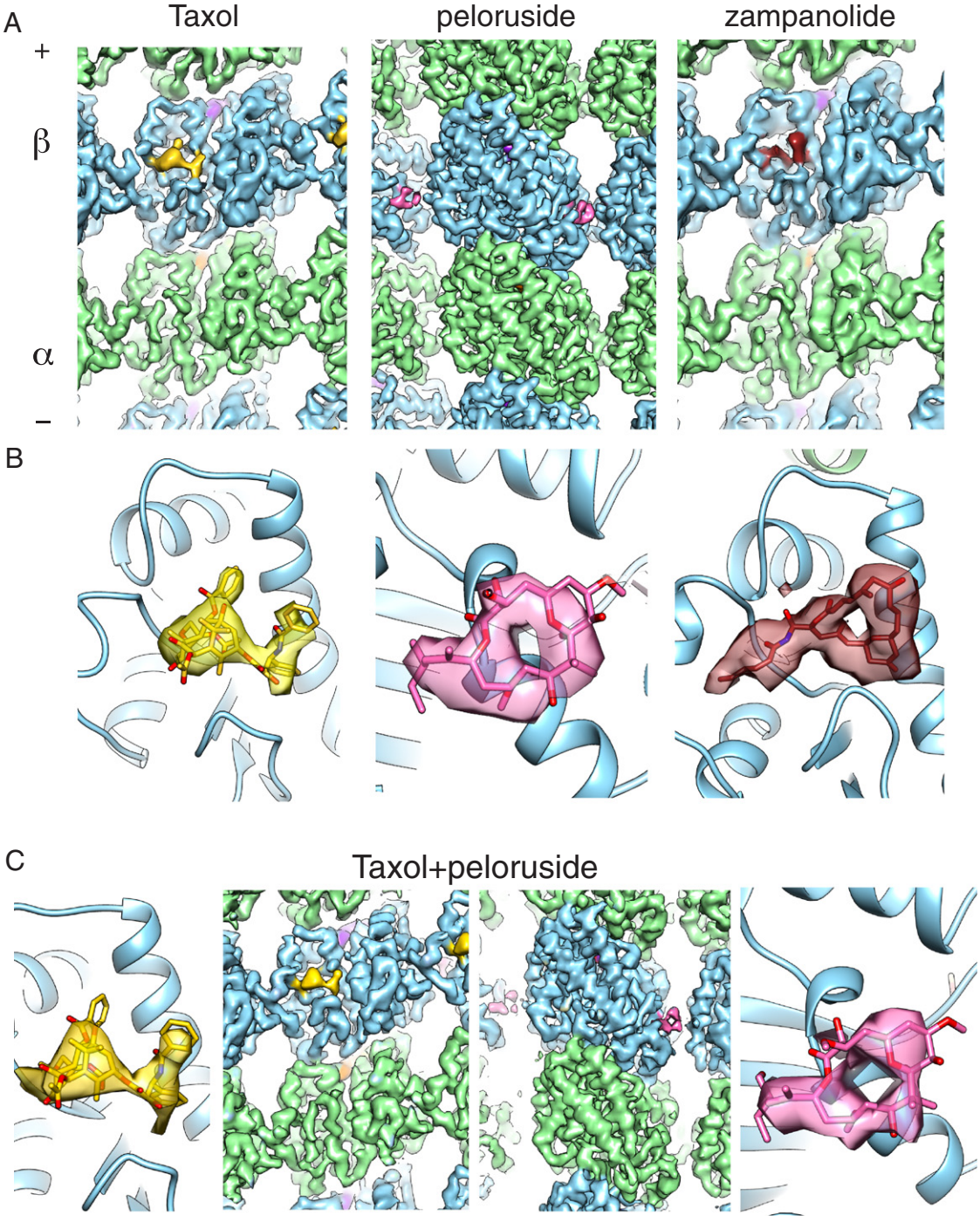

Fig. 2. Cryo-EM reconstructions and MSA binding pockets. (A) Structures for MTs bound to Taxol (at 3.9 Å resolution, left), peloruside (3.9 Å, middle), and zampanolide (4.2 Å, right). Taxol- and zampanolide-bound MTs are seen from the lumen, peloruside-MT from the exterior. (B) Drug-binding sites showing the segmented densities for the MSA molecules. (C) Lumen and exterior view of an MT doubly bound to peloruside and Taxol (4.1 Å resolution, middle). The Taxol and peloruside binding pockets are shown on the left and right, respectively.

zampanolide, focusing specifically on the structural effect of adding the drugs to preformed MTs (due to the limiting amount of drug). We found that the zampanolide-MT reconstructions have a similar axial repeat to that of those bound to Taxol (81.6 Å *versus* 81.8 Å) and to drug-free MTs (81.5 Å;Table S1). Peloruside, which binds to a pocket on the MT exterior (Fig. 1), results in an axial repeat of 81.0 Å. This difference in MT lattice parameters suggests that zampanolide and Taxol stabilize MTs via a mechanism distinct from that of peloruside.

Reconstruction features of drug-stabilized MTs

We obtained near-atomic (3.9–4.2 Å overall) resolution cryo-EM reconstructions for Taxol-MT (3.9 Å), peloruside-MT (3.9 Å), doubly bound (Taxol and peloruside-MT;4.1 Å), and zampanolide-MT structures (4.2 Å)(Fig. 2 and Fig. S1). Resolution estimates were calculated on the reconstructions of whole MT segments after imposing pseudo-helical symmetry, as previously described [18]. β-strand separation, helical ridges along alpha helices, and side-chain densities are visible throughout the majority of the reconstructions (Fig. S2A), as expected for the estimated resolution range. Densities for all drug ligands are sufficiently resolved to conclude that their binding sites agree with those visualized in previous X-ray crystallographic studies carried out outside of the MT context [24,25,33] (Fig. 2).

The Taxol-MT and the peloruside-MT reconstructions have similar overall resolution, in spite of the fact that the dataset for Taxol was larger (~23,000 Taxol-MT segments *versus* ~16,000 peloruside-MT segments—see Supplementary Materials and Methods for details;Fig. S1). Furthermore, while in the Taxol-MT cryo-EM map the luminal surface, including the Taxol-binding site, is well-defined (Fig. 2), other tubulin regions, like the MT outside surface or the β-sheet parallel to the helical axis, appear more poorly resolved (Fig. S2), indicative of anisotropic resolution. The same is true of the zampanolide-MT reconstruction. The taxane reconstructions (Taxol-MT and zampanolide-MT) have very different local resolution distributions from those of the drug-free or peloruside-MT reconstructions (Fig. 3 and Fig. S3). This difference is most striking concerning the motor domain of kinesin in the Taxol-MT and zampanolide-MT reconstructions, for which resolution is significantly worse (5–5.5 Å) than for tubulin (3.5–4 Å). In contrast, the peloruside-MT and peloruside-Taxol-MT reconstructions have more uniform resolution throughout the structure (Figs. 3A and Fig. S3), similar to what is seen for drug-free MTs [18]. The lower resolution of the decorating kinesin in the Taxol-bound structure is not attributable to low kinesin occupancy, which we estimate is ≥90% for all but one of our Taxol datasets (Supplementary Materials and Methods and Table S2). Instead, either the attachment of kinesin is more flexible or the MT helical lattice is less ordered. The latter would lead to the averaging of slightly different helical arrangements and ultimately result in propagating alignment errors that would blur the density map, especially at higher radii. In either case, our observation is relevant to structural and biophysical studies characterizing the interaction of kinesin and other MAPs with MTs, which often use Taxol to render MTs resistant to temperature changes and devoid of dynamic instability.

Taxol-site binders result in lattice heterogeneity

To test for the possibility of conformational heterogeneity in the MT lattice, we used RELION to carry out 3D classification of the Taxol-MT, the peloruside-MT, the zampanolide-MT, and the drug-free MT datasets (see Supplementary Materials and Methods for details). The resulting 3D classes for both of the MTs stabilized by Taxol-site drugs (Taxol-MT and zampanolide-MT) have visible deformations from a perfectly circular cross-section of the MT wall that are not apparent in the peloruside-MT or the drug-free 3D classes (Movie S1). We quantify the deformations in the MT walls by taking projections of the resulting 3D class volumes along the helical axis and computing elliptical parameters for a set of coordinates representing the center of each PF in the MT (See Supplementary Materials and Methods for details). The coordinates are then fit to the equation for an ellipse. The resulting short-axis/long-axis ratio represents the degree to which the MT-PF arrangement, within a given 3D class volume, deviates from an idealized, circular MT cross-section. A perfectly circular MT would produce a ratio of 1, since the long axis and short axis would be equal. We find that the 3D classes corresponding to the peloruside-MT or drug-free MTs (Fig. 3C) have a small spread of ratios (homogeneous population) and are close to 1 ("circular" cross-section). However, the 3D classes for Taxol and zampanolide MTs show a wider range of "elliptical" and continuous deformations in the MT wall (Fig. 3B–C) that correspond to ~1–2 Å displacement in the position of tubulin subunits, indicating that the MT walls are more deformable and more heterogeneous in comparison to the peloruside-MT or drug-free 3D classes. This finding suggests that the observed conformational heterogeneity is due to MT-wall flexibility induced by the binding of a drug to the Taxol site.

Taxol-site binders share common tubulin interactions

The binding to tubulin of both Taxol and zampanolide has been characterized previously in the context of an aberrant polymer (zinc-induced 2D sheets) by electron crystallography for the former [33] and in the context of unassembled tubulin by

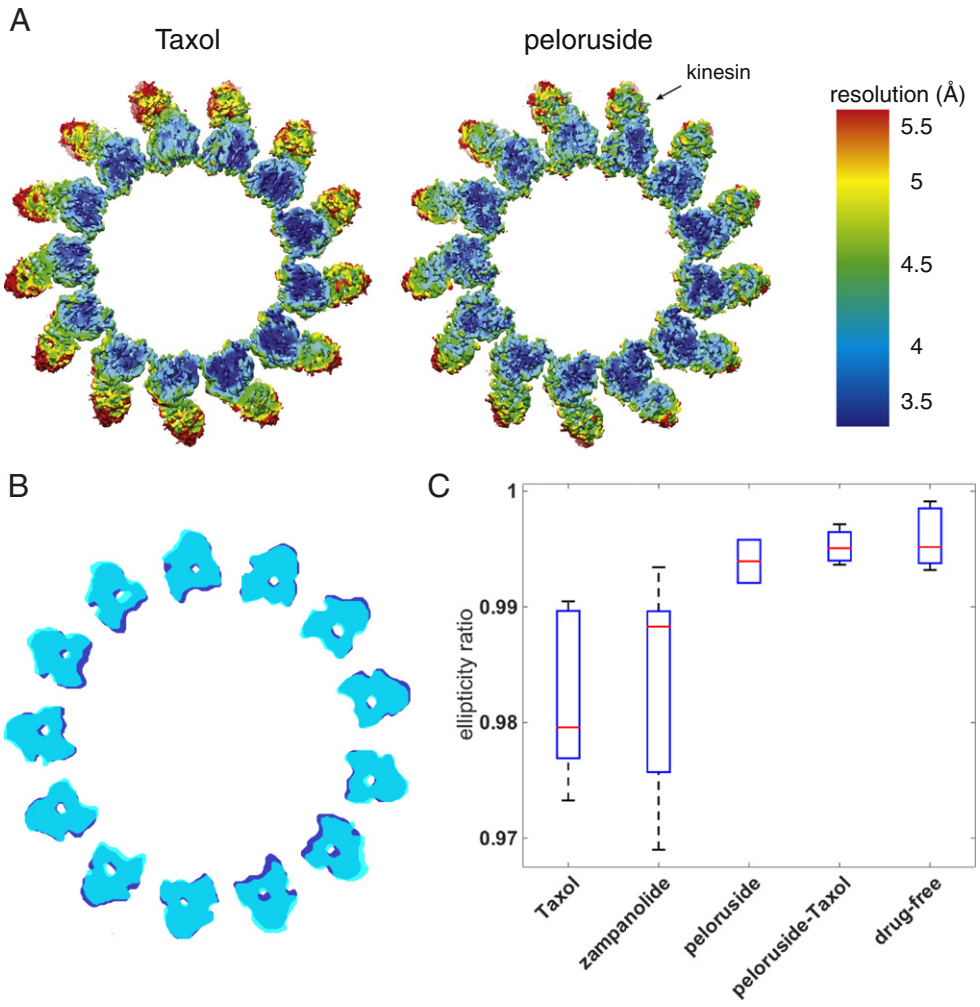

Fig. 3. Taxol and zampanolide induce MT wall flexibility. (A) End-on view of the cryo-EM reconstructions of Taxol-bound MTs (left) and peloruside-bound MTs (right). The decorating kinesin, used as a fiducial for the alignment of αβ-tubulin dimers, is visualized at significantly lower resolution in the Taxol sample (5–5.5 Å) *versus* peloruside sample (4–4.5 Å), likely due to alignment errors resulting from wall deformations in the MTs. Regions for which the local resolution of the decorating kinesin differs significantly are boxed. (B) End-on view of two representative MT classes from the Taxol-bound (added post-lattice formation) MT sample obtained using RELION 3D sorting. (C) The deformations of the MT wall from a circular cross-section were approximated as ellipses. The parameters of the elliptical fits to the different 3D classes are displayed as a ratio between the long and short axes of the ellipse, where a ratio of 1 corresponds to a circle. The red line indicates the median value, the blue box indicates the 25th and 75th percentiles, and the black lines indicate range of values for each dataset (n = 5).

X-ray crystallography for the latter [24]. Here, we reexamine the modeled interactions between these two Taxol-site drugs in the context of the physiological tubulin polymer, the MT, using our cryo-EM reconstructions. We will refer to the functional groups of Taxol and zampanolide using their numbered carbon atoms (Fig. 1).

The Taxol density is clearly defined in the density map (Fig. 2B, left) and agrees well with previous models of Taxol bound to zinc-induced tubulin sheets [33,34]. Our cryo-EM-based atomic model defines three critical interactions between tubulin and Taxol that are well supported by previous pharmacophore studies (Fig. 4A). First, there are extensive van der Waals interactions between the 3′-benzoyl of Taxol, which has been previously shown to be essential for Taxol's stabilizing activity [35], and β-tubulin H229 (Fig. 4A). Additionally, the nitrogen in β-H229 is appropriately positioned to make a hydrogen bond with Taxol's 3′-oxygen. Second, studies on synthetic Taxol analogs demonstrated that the 2′-OH group is crucial to Taxol's activity [35,36]. Removal of this group causes a 2 orders of magnitude reduction in binding affinity [35]. We find that Taxol's 2′-OH is close enough to hydrogen bond with the backbone carbonyl of R369. The final interaction involves the β-tubulin backbone

NH of T276 (in strand S7) making a hydrogen bond with Taxol's oxetane ring, a group that has also been shown to be critical for Taxol's stabilizing activity. Other functional groups, such as the C10 acetyl group and the C4 acetate, which are less critical for Taxol's activity [36], do not appear to interact with tubulin in our model. The C13 side chain, which is widely reported to be critical but has also been heavily modified in pharmacological studies [37], is found to interact with helix H7 by providing hydrophobic contacts, particularly with β-H229, which may explain why hydrophobic substitutions are tolerated at this site. These findings are all consistent with the Taxol-binding pocket described in the electron crystallographic structure [33]. Interestingly, neither the map density nor the refined atomic models seem to support direct contacts between Taxol and the M-loop (Figs. 2A and 4A) in the MT. A lack of contribution of the M-loop to Taxol binding/activity is consistent with Taxol binding and stabilization of zinc-induced tubulin sheets, in which the M-loop, which coordinates the zinc ion, is in a totally different conformation from that observed in the context of the MT lattice.

Although the zampanolide reconstruction has lower resolution (4.2 Å *versus* 3.9 Å), clear density corresponding to zampanolide is visible, and its binding site location is in agreement with that reported in the crystal structure [24]. Density for the full ring can only be seen at low density thresholds (Fig. 2B, right), perhaps due to the inherent flexibility of the C1–C4 portion, which has been shown to have correspondingly higher crystallographic *B*-factors [24,38]. Similar to Taxol, and consistent with crystallographic studies [24], zampanolide makes specific contacts with β-H229 (through covalent bonding) and β-T276 (through hydrogen-bonding interactions with the *N*-acyl hemiaminal group of zampanolide;Fig. 4B), but it does not appear to interact directly with the M-loop.

We next compare the refined atomic models corresponding to the two Taxol-site drugs, Taxol and zampanolide, specifically focusing on the structural differences around the binding pocket. Taxol binding appears to give rise to subtle changes in the loops surrounding the binding pocket when compared to the drug-free atomic model, most significantly in the S9–S10 loop (0.53 Å Cα rmsd), which moves down toward the N-site (Fig. 4C); the M-loop moves toward the Taxol molecule, and the H6–H7 loop moves away from Taxol. In contrast, upon zampanolide binding, the S9–S10 loop appears to close slightly inward, and the M-loop adopts a "pushed out" position with respect to both the drug-free model and the Taxol-bound model. These differences indicate that while the two drugs bind the same binding pocket in β-tubulin, their different structure results in slight differences local to the binding site, although these differences do not seem to affect MT lattice parameters.

Peloruside binding affects MT wall curvature, resulting in a less distinctive seam structure

A previous crystal structure [25] revealed that peloruside binds at a site that would position it near the lateral interface between PFs on the MT exterior (Fig. 1). Our cryo-EM structure further confirms that proposal. As mentioned before, comparison of the drug-free MT cryo-EM reconstruction [18] with the peloruside-MT reconstruction reveals a small change in axial repeat (81.0 Å *versus* 81.5 Å; peloruside *versus* drug-free) that originates from an apparent

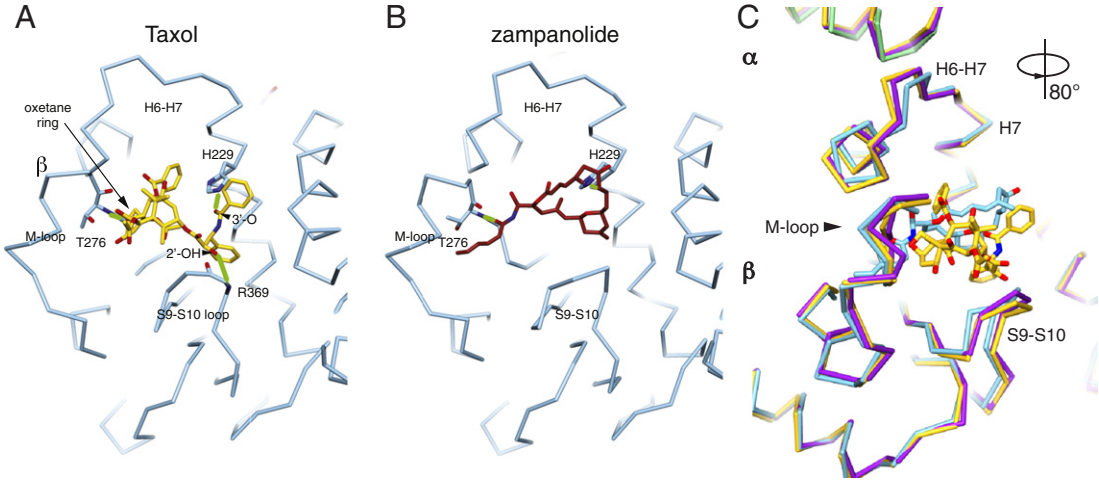

Fig. 4. Comparison of the Taxol- and zampanolide-binding pockets. (A) Taxol-binding pocket with three critical tubulin–Taxol interactions marked by the solid green lines. Two of these critical contacts are shared with zampanolide. (B) Zampanolide-binding site highlighting interactions with T276 and H229 (marked with green lines) shared with Taxol. (C) Superposition of the refined atomic models for Taxol-bound (gold), drug-free (purple), and zampanolide-bound MT (blue, with α-tubulin shown in green).

slight compaction of β-tubulin (Table S1). Given the position of peloruside near the lateral contacts (Fig. 2A, center), we next looked at its effects on this interface. When imposing pseudo-helical symmetry (see Supplementary Materials and Methods) [11,18,39], we necessarily miss any structural changes that may occur at the seam, the point where helical symmetry breaks in the MT lattice. By calculating unsymmetrized (C1) reconstructions, we previously showed [18] that drug-free MTs, irrespective of their nucleotide state, deviate from a perfect cylindrical arrangement due to the fact that PFs on either side of the seam are further apart from each other and are slightly rotated with respect to the rest of the PFs. We find that the drug-free and peloruside-bound MT C1 reconstructions are very distinct at the seam (Fig. 5A and Movie S2). The difference in angle relating to PFs across the seam in the peloruside-MT reconstruction is smaller by 3°, and the PFs flanking the seam come closer together, moving >2 Å (Cα rmsd) toward the MT lumen. As a consequence, the lateral contact at the seam is more like those at homotypic contacts, with just ~1 Å (Cα rmsd) average difference between helical and C1 reconstructions at the seam (Fig. 5A, right). In other words, the peloruside MT structure is more cylindrical than the drug-free MT states.

Although the C1 reconstruction is of lower resolution (4.6 Å), clear density attributable to peloruside can be seen at every binding pocket, including the one adjacent to the seam (Fig. 5B, compare left and right). Although we cannot distinguish between mechanisms in which peloruside binding would exert this effect in MT lattice regularization via a dominant alteration in the heterotypic seam interactions or in the homotypic lateral contacts, our current analysis shows that the largest structural changes occur at the seam, indicating that peloruside's most prominent effect may be to stabilize the MT by promoting interactions between PFs across to the seam. The homotypic and heterotypic lateral interactions obtained from the docking of our atomic model of the peloruside-bound PFs are indistinguishable at the present resolution (Fig. 5B).

The effect of peloruside on lateral contacts and seam "regularization" is reminiscent of that seen for MTs bound to the +TIP protein EB3 [18]. While EB3 binds across non-seam lateral interfaces but not at the seam, it results in an angle between PFs that ultimately repositions those involved in lateral contacts at the seam, generating a more cylindrical pattern. The results now obtained for peloruside further support the idea that the seam may be a weak point within the MT lattice and that its "cylindrical regularization" by peloruside may result in MT stabilization.

Peloruside overrides the effects of Taxol binding

Previous studies have proposed that drugs binding to the Taxol site can biochemically synergize with drugs that recognize an alternative binding-site, such as peloruside or laulimalide [30,31]. Additionally, previous crystal structures of peloruside and epothilone simultaneously bound to tubulin identified a novel hydrogen-bonding network that was proposed to be due to allosteric cross-talk between the two binding sites [25]. We therefore wondered whether a peloruside-Taxol doubly bound MT structure would be more similar to either the singly bound Taxol-MT or the peloruside-MT structures, or an intermediate between the two. To address this question, we obtained a reconstruction of the doubly bound peloruside-Taxol-MT at 4.1-Å resolution (Fig. 2). The overall resolution of the doubly bound reconstruction is slightly worse than that of the Taxol-MT reconstruction (3.9 Å), likely due to the fact that the dataset for the former was considerably smaller (12,014 *versus* 21,757 particles; Fig. S1). We find that the doubly bound peloruside-Taxol-MT has an axial repeat intermediate between that of the singly bound peloruside and Taxol structures (81.5 Å) that originates from intermediate values for both the intra- and interdimer distances (Table S1). There is no detectable difference in structure, at our present resolution, around the binding pockets for both Taxol and peloruside in the doubly bound MT compared with the singly bound structures (Fig. 2, bottom panel), and the critical interactions between the tubulin and these small molecules remain seemingly unchanged in the doubly bound state. Interestingly, the peloruside-Taxol-MT structure shows a "closed" seam in the unsymmetrized reconstruction, similar to the effect observed for peloruside alone, and more closely approximates an ideal cylindrical PF arrangement (Fig. S4). Additionally, the reconstruction does not suffer from the lattice heterogeneity observed in Taxol-MTs (Figs. 3C, S2, and S3), suggesting that the effects of peloruside override the effects of Taxol with regard to lateral interactions.

Biochemical cross-talk between the taxane and peloruside binding sites

While some biochemical studies have suggested a synergistic biochemical effect between Taxol and peloruside binding site ligands [30,31,40], other studies [41] show little to no influence of laulimalide binding (which binds at the peloruside site) on the affinity of Flutax-2 (a bona fide fluorescent paclitaxel binding site probe) for the taxane site. Since our structure of the doubly bound MT indicates a dominant effect of peloruside over Taxol, we decided to further investigate a possible synergy between peloruside and Taxol-site binders in their binding affinity to MTs that could be due to communication between the two binding sites.

The influence of epothilone A (a bona fide taxane-site ligand) [42] on the binding of peloruside to MTs was determined by measuring the binding

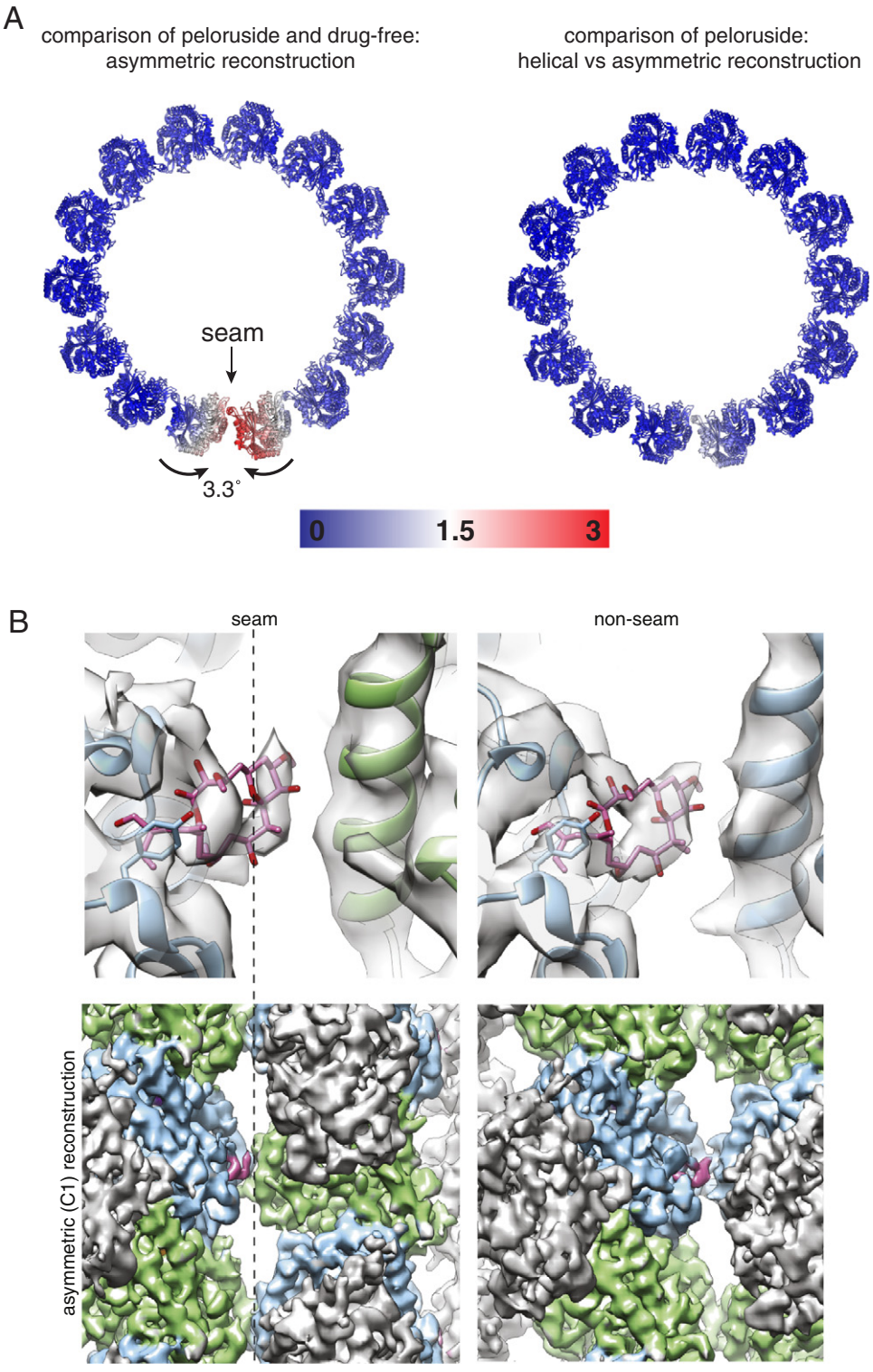

Fig. 5. Structural changes in the MT upon peloruside binding. (A) Cα atoms RMSD (indicated in colors ranging from blue to red) between atomic models of one helical turn of tubulin dimers for the C1 reconstructions of drug-free and peloruside-bound MTs (left) and for the pseudo-helically averaged and the asymmetric (C1) reconstructions for peloruside-bound MTs (right). The red color by the seam reflects the changes in PF orientation that give rise to seam closure in the presence of peloruside. The changes are minimal when comparing C1 and helical peloruside reconstructions, indicating that the peloruside-bound MTs are approximated well by an ideal helical arrangement of PFs. (B) Peloruside density is visible at both seam and non-seam binding pockets in the asymmetric (C1) reconstruction, indicating that peloruside has no preference for homo-(β-β) or hetero-(α-β) tubulin interactions (top panel contains magnified views of bottom ones).

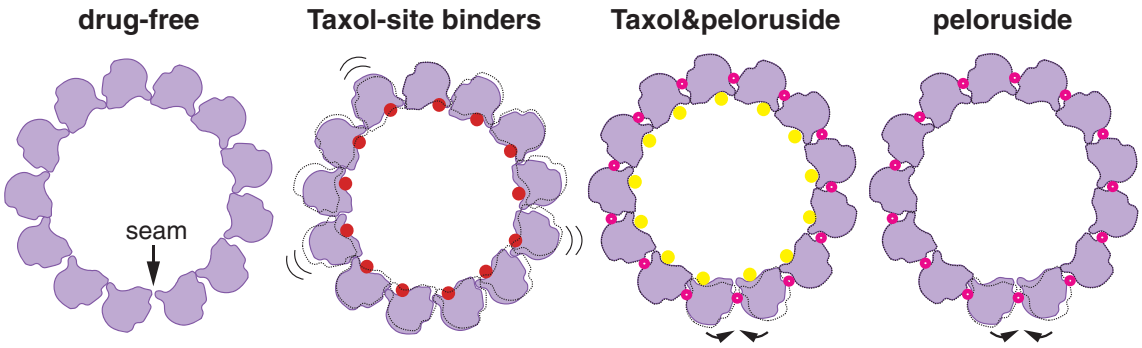

Fig. 6. Schematic summary of the changes in MT structure induced by MSA binding. Taxol and zampanolide (both Taxol-site binders) induce lattice heterogeneity (second from left), whereas peloruside promotes a "closed" seam structure through changes in the lateral contacts that are most notable at the seam (right). Peloruside overrides the effect of Taxol, resulting in a more ordered lattice and a "closed" seam structure (second from right).

constant of peloruside to stabilized and crosslinked MTs, both with the taxane binding site empty and with the taxane binding site saturated with epothilone A. We observed no significant differences between the binding constant determined in the absence ($3.2 \pm 0.8 \times 10^6$ M^{-1}) or in the presence of epothilone A ($3.5 \pm 0.4 \times 10^6$ M^{-1}). Reciprocally, the binding constant of epothilone A was unaffected by the presence of peloruside ($8.1 \pm 0.4 \times 10^7$ M^{-1} in the absence of peloruside *versus* $7.5 \pm 1 \times 10^7$ M^{-1} in the presence of peloruside), confirming the observation of Pryor *et al.* [41].

Discussion

Our cryo-EM studies demonstrate that the MSAs Taxol, zampanolide, and peloruside have distinct effects on the MT lattice, indicating different stabilization mechanisms. Using 3D classification, we have identified structural heterogeneity around the MT wall that is only observed in the presence of Taxol or zampanolide, which binds to the same taxane site on β-tubulin (Fig. 6). We infer that this structural heterogeneity is due to a small and likely continuous variation of the lateral contacts between PFs that ultimately limits the resolution and interpretability of the cryo-EM reconstructions. This structural flexibility parallels the greater mechanical flexibility observed for Taxol-stabilized MTs [14,43].

The MT flexibility induced by Taxol and zampanolide may be inherent to their mechanism of stabilization, as has been suggested by molecular dynamic simulations [44]. Taxol-site binding appears to effectively allow, if not promote, a wider range of conformations of the lateral contacts without resulting in MT disassembly. A possible explanation may be that more uniform lateral interfaces are produced when the drug-free MT is under tension due to the tendency of the tubulin dimer to curve outwards. Taxol has been shown to straighten PFs [17] (no information is available for zampanolide), and thus, a Taxol-MT lattice will not be under the tension that would otherwise restrict motions. It is important to note that neither Taxol nor zampanolide forms direct contacts with the M-loop involved in lateral contacts. However, they both establish two critical interactions with tubulin: a hydrogen bond to the nitrogen backbone of T276 (immediately preceding the M-loop) and critical contacts with H229 in the H7 "core helix". The functional groups that form these contacts are known to be critical for the MT-stabilizing activity of both drugs.

One open question regarding Taxol-site binders is whether they affect the MT lattice differently, given that they display a wide range of structural motifs. Our structures show that Taxol and zampanolide, two structurally divergent taxane-site binders, affect the binding pocket in a distinct manner, but without resulting in differences on the MT lattice. We find that binding of Taxol results in the expansion of the taxane binding pocket, while zampanolide binding results in its tightening, a reflection of the distinctly different molecular shapes of these two ligands: Taxol is larger, taking up more space, hence the expansion of the pocket, and zampanolide is smaller and more compact, hence the tightening of the pocket. In spite of these differences, two crucial contacts between tubulin and ligandare preserved in the binding modes of Taxol and zampanolide, namely those with β-tubulin residues T276 and H229.

In contrast to Taxol and zampanolide, peloruside-MTs do not exhibit detectable increased heterogeneity with respect to unbound MTs. Thus, peloruside-stabilized MTs should be more suitable substrates for MT-MAP structural studies. Peloruside seems to act predominantly through strengthening lateral contacts and altering those at the seam, regularizing the lattice to more closely resemble a helical structure (Fig. 5). In this respect, peloruside seems to function similarly to the plus end binding protein EB3. Both bind between

PFs and cause the closure of the seam. These findings support a model in which the seam may be a weak point within the MT lattice. Interestingly, in the doubly bound structure analyzed here, the effect of peloruside on lateral contact regularization is dominant over the increased flexibility that Taxol causes on its own. This results in a more helical arrangement of PFs, similar to what is seen for singly bound peloruside MTs (Fig. 6).

These results and the lack of influence of peloruside on epothilone A binding to MTs (or vice versa) cannot explain the cooperative cytotoxicity effects observed between laulimalide site and taxane-site drugs. However, in cell assays for cytotoxicity that show cooperative effects [31,45,46], the intracellular ratio of tubulin to drug is around 100:1 or 50:1, while in our structural and biochemical studies, the proportion is typically 1:1. Given the fact that peloruside binding has no effect on taxane binding and vice versa, the chances that a single tubulin molecule in the cell has both a molecule of peloruside and another of taxane bound are far below 1%. Thus, simultaneous binding cannot be the reason for the synergistic effect observed in the cellular context. We propose that the synergy in cytotoxicity is likely to come from the different structural effects of the drugs bound at different points along the MT lattice, which could produce an additive effect on MT stability, rather than from simultaneous binding of both drugs to a single tubulin molecule.

The results reported here highlight the complex structural responses of the MT lattice to differences in small-molecule structure and binding. Further work will be required to understand the details of the mechanisms involved in MT stabilization, especially for compounds that bind the taxane site. However, our finding that the addition of taxane-site agents to MTs induces lattice heterogeneity is of immediate relevance to studies of the interaction of MAPs with MTs. Taxol is commonly used to stabilize MTs in biophysical and structural analyses of motors and other MT partners, and the MT heterogeneity we have described here needs to be factored in when interpreting data on MAP-binding or motor protein motility parameters. In fact, researchers may consider using MT stabilizers like peloruside, or non-hydrolyzable GTP analogs, if they are concerned with the possibility that the Taxol-induced flexibility in the MT lattice could complicate their conclusions.

Materials and Methods

MT assembly and vitrification

MT samples varied in terms of when stabilizing drugs were added (either before or after polymerization; Table S1). For each set of conditions, MTs were prepared from porcine tubulin (Cytoskeleton) at a final concentration of 0.5 mg/mL (~45 μM) and a final drug:tubulin molar ratio of 1.5:3. The formed MTs were pelleted and then resuspended in EM buffer containing the desired drug. In the case of the doubly bound structure, the MT pellet was first resuspended in peloruside-containing EM buffer, and then Taxol was added after approximately 1 min. Due to the very small amounts of available zampanolide, a slightly different protocol was used (see Supplementary Materials and Methods). MTs were decorated with kinesin to aid the alignment of α- and β- tubulin monomers and to localize the seam. Sample vitrification and automatic data collection on a low base Titan microscope (FEI) equipped with a K2 summit camera (Gatan) were performed as described previously [18,39] (see Supplementary Materials and Methods for details).

Image processing

Image processing followed procedures described previously [11,18,39]. Briefly, MT segments along the length of a MT were boxed out using overlapping boxes, each box separated by 80 Å. Global alignment parameters were obtained against low-pass filtered (~20 Å) references, comprising 12–15 PF MT models. These parameters were used as inputs for refinement in FREALIGN [47]. In order to characterize the structural heterogeneity in each dataset, we employed RELION 3D classification [48]. See the Supplementary Materials and Methods for further details.

Model building

The experimental density maps were sharpened using *B*-factors of 125–150 $Å^{-1}$ and filtered to the estimated resolution using the gold-standard FSC (Fourier shell correlation). We used as starting atomic model that of the dynamic and GDP-bound state without drug from our previous work (PDB: 3JAS) [18]. Ligand conformations were copied from high-resolution crystal structures (see Supplementary Materials and Methods) and were kept fixed, but rigid-body translations/rotations were optimized. A 3 × 3 dimer section of the MT lattice was modeled using Rosetta refinement [49] as described previously [11] (see also Supplementary Materials and Methods). The lowest 1% energy models by total score were selected, and a consensus model was created by averaging backbone coordinates and selecting the most common rotamer. This representative model was then refined against the map using refmac [50] to produce a final model with optimal geometry and to fit to the map (see also Supplementary Materials and Methods). The final models typically deviated from the initial and starting model by less than 0.5 Å rmsd.

MT-MSA binding affinity

The binding affinity for MTs of epothilone A, a taxane-site binder, and peloruside, which binds far

from the taxane site, has already been well characterized [27,42]. In order to determine whether the binding of peloruside to MTs is allosterically affected by the occupancy of the distant taxane site, we measured the binding affinity of peloruside to MTs, both in the presence or absence of saturating amounts of epothilone A. We followed procedures previously described in detail that measure the affinity of antimitotic agents for crosslinked, stabilized MTs using centrifugation and HPLC [27,51]. Crosslinked MTs (obtained following previously described procedures [52]) at a concentration of 0.6 μM tubulin in GAB buffer [3.4 M glycerol, 10 mM sodium phosphate, 1 mM EGTA, and 6 mM $MgCl_2$ (pH 6.5)] were incubated for 30 min at 25 °C with 0.1 mM GTP and 10 μM of epothilone A in order to saturate them with this drug (binding constant of epothilone A for MTs is $7.5 \pm 1 \times 10^7$ M^{-1} [42]). Unligated MTs were incubated for the same time with an equivalent volume of DMSO (dimethyl sulfoxide). Peloruside (0.1–10 μM) or an equivalent volume of DMSO was then added to the samples, followed by a further incubation for 30 min at 25 °C. The samples were then centrifuged for 20 min at 25 °C at 50,000 rpm in a TLA 120.2 rotor (1 ml per sample) in an Optima TLX centrifuge (Beckman, Palo Alto, CA) to separate the MTs from the unligated peloruside. The MT-containing pellets were resuspended in 10 mM NaPi. An internal standard of 10 μM docetaxel was added to all resuspended pellets and supernatants, and peloruside and docetaxel extracted three times with one reaction volume of CH_2Cl_2. The extracts were dried and the samples resuspended in 35 μL (vol/vol) 55% methanol in water. The amount of compounds was analyzed using an Agilent 1100 Series instrument employing a Supelcosil, LC18 DB HPLC column of dimensions 250 × 4.6 mm and a bead diameter of 5 μm. The column was developed with a gradient of 13-min 55% methanol in water, 10-min 70% methanol in water, and 10-min 55% methanol in water at a flow rate of 1 mL/min. The absorbance was monitored at 205 and 230 nm, and the content of peloruside in the pellets (bound to MTs) and in the supernatant (free) was determined by comparison with the known concentration of docetaxel, which is used as standard. The binding constant of peloruside was then calculated employing EQUIGRA V5.0 [52] and compared to both unligated and epothilone-ligated MTs.

We measured the influence of peloruside on the binding of epothilone A to MTs similarly, except that five tubes (5 ml) of each sample were processed, mixed, and extracted simultaneously to compensate for the lower concentrations of epothilone A needed, given the higher binding constant of this compound. MTs fully saturated with peloruside were obtained by incubating stabilized and crosslinked MTs (50 nM) for 30 min at 25 °C, in GAB buffer containing 0.1 mM GTP with 50 μM of peloruside (binding constant for MTs $3.2 \pm 0.8 \times 10^6$ M^{-1} [27]). As before, unligated MTs were incubated with an equivalent volume of DMSO. Epothilone A (0.002 to 1 μM) or an equivalent volume of DMSO was then added to the samples, followed by a further incubation for 30 min at 25 °C. The binding constant of epothilone A was then determined as described above, except that the extracts were dried and the samples resuspended in 35 μL (vol/vol) 70% methanol in water, and the column was developed isocratically for 30 min with 70% methanol in water at a flow rate of 1 ml/min and 10 min 55% methanol in water at 1 mL/min. The absorbance was monitored at 220 and 260 nm.

Accession numbers

All electron density maps have been deposited in the EMDB accession numbers EMD-8320, EMD-8321, EMD-8322, and EMD-8323. Atomic models are deposited in the PDB accession numbers 5SYC, 5SYE, 5SYF, and 5SYG.

Supplementary data to this article can be found online at http://dx.doi.org/10.1016/j.jmb.2017.01.001.

Acknowledgments

We thank Tom Houweling and Patricia Grob for computational and EM support, respectively; Sjors Scheres for valuable help on RELION; Frank Dimaio and Ray Wang for advice on Rosetta; and Rui Zhang for helpful comments on MT image analysis. We gratefully acknowledge the National Energy Research Scientific Computing Center, a DOE Office of Science User Facility supported by the Office of Science of the U.S. Department of Energy under Contract No. DE-AC02-05CH11231, for providing computational resources. This work was funded by NIH grant GM51487 (K.H.D., E.N.) and grants BIO2013-42984-R from Ministerio de Economia y Competitividad and S2010/BMD-2457 BIPEDD2 from Comunidad Autónoma de Madrid (J.F.D.). The authors acknowledge the networking contribution by the COST Action CM1407 “Challenging organic syntheses inspired by nature - from natural products chemistry to drug discovery” and the COST action CM1470. E.N. is a Howard Hughes Medical Institute Investigator.

Received 12 October 2016;
Received in revised form 30 December 2016;
Accepted 3 January 2017
Available online 17 January 2017

Keywords:
cryo-EM;
microtubule;
microtubule-stabilizing agents;
Taxol;
peloruside;
zampanolide

Present address: S. Howes, Department of Molecular Cell Biology, Leiden University Medical Center, 2333 ZC Leiden, Netherlands.

Abbreviations used:
MT, microtubule; PF, protofilament; MAP, MT-associated protein; MSA, MT-stabilizing agent; EM, electron microscopy; GTP, guanosine triphosphate; GDP, guanosine diphosphate; FSC, Fourier shell correlation; DMSO, dimethyl sulfoxide.

References

[1] T. Mitchison, M. Kirschner, Dynamic instability of microtubule growth, Nature 312 (1984) 237–242.
[2] A. Akhmanova, M.O. Steinmetz, Control of microtubule organization and dynamics: two ends in the limelight, Nat. Rev. Mol. Cell Biol. 16 (2015) 711–726.
[3] E. Nogales, R. Zhang, Visualizing microtubule structural transitions and interactions with associated proteins, Curr. Opin. Struct. Biol. 37 (2016) 90–96.
[4] P.B. Schiff, J. Fant, S.B. Horwitz, Promotion of microtubule assembly *in vitro* by taxol, Nature 277 (1979) 665–667.
[5] J.J. Manfredi, S.B. Horwitz, Taxol: an antimitotic agent with a new mechanism of action, Pharmacol. Ther. 25 (1984) 83–125.
[6] J.J. Field, A. Kanakkanthara, J.H. Miller, Microtubule-targeting agents are clinically successful due to both mitotic and interphase impairment of microtubule function, Bioorg. Med. Chem. 22 (2014) 5050–5059.
[7] M.C. Wani, H.L. Taylor, M.E. Wall, P. Coggon, A.T. McPhail, Plant antitumor agents. VI. The isolation and structure of taxol, a novel antileukemic and antitumor agent from *Taxus brevifolia*, J. Am. Chem. Soc. 93 (1971) 2325–2327.
[8] I. Ojima, K. Kumar, D. Awasthi, J.G. Vineberg, Drug discovery targeting cell division proteins, microtubules and FtsZ, Bioorg. Med. Chem. 22 (2014) 5060–5077.
[9] E. Nogales, S.G. Wolf, K.H. Downing, Structure of the alpha beta tubulin dimer by electron crystallography, Nature 391 (1998) 199–203.
[10] E. Nogales, M. Whittaker, R.A. Milligan, K.H. Downing, High-resolution model of the microtubule, Cell 96 (1999) 79–88.
[11] G.M. Alushin, G.C. Lander, E.H. Kellogg, R. Zhang, D. Baker, E. Nogales, High-resolution microtubule structures reveal the structural transitions in alphabeta-tubulin upon GTP hydrolysis, Cell 157 (2014) 1117–1129.
[12] R.H. Wade, D. Chretien, D. Job, Characterization of microtubule protofilament numbers. How does the surface lattice accommodate? J. Mol. Biol. 212 (1990) 775–786.
[13] D. Chretien, F. Metoz, F. Verde, E. Karsenti, R.H. Wade, Lattice defects in microtubules: protofilament numbers vary within individual microtubules, J. Cell Biol. 117 (1992) 1031–1040.
[14] H. Sui, K.H. Downing, Structural basis of interprotofilament interaction and lateral deformation of microtubules, Structure 18 (2010) 1022–1031.
[15] I. Arnal, R.H. Wade, How does taxol stabilize microtubules? Curr. Biol. 5 (1995) 900–908.
[16] J.F. Diaz, J.M. Valpuesta, P. Chacon, G. Diakun, J.M. Andreu, Changes in microtubule protofilament number induced by Taxol binding to an easily accessible site. Internal microtubule dynamics, J. Biol. Chem. 273 (1998) 33,803–33,810.
[17] C. Elie-Caille, F. Severin, J. Helenius, J. Howard, D.J. Muller, A.A. Hyman, Straight GDP-tubulin protofilaments form in the presence of taxol, Curr. Biol. 17 (2007) 1765–1770.
[18] R. Zhang, G.M. Alushin, A. Brown, E. Nogales, Mechanistic origin of microtubule dynamic instability and its modulation by EB proteins, Cell 162 (2015) 849–859.
[19] K. Gerth, N. Bedorf, G. Hofle, H. Irschik, H. Reichenbach, Epothilons A and B: antifungal and cytotoxic compounds from *Sorangium cellulosum* (Myxobacteria). Production, physico-chemical and biological properties, J. Antibiot. (Tokyo) 49 (1996) 560–563.
[20] J.-I. Tanaka, T. Higa, Zampanolide, a new cytotoxic macrolide from a marine sponge, Tetrahedron Lett. 37 (1996) 5535–5538.
[21] L.M. West, P.T. Northcote, C.N. Battershill, Peloruside A: a potent cytotoxic macrolide isolated from the New Zealand marine sponge Mycale sp. J. Organomet. Chem. 65 (2000) 445–449.
[22] E. ter Haar, R.J. Kowalski, E. Hamel, C.M. Lin, R.E. Longley, S.P. Gunasekera, et al., Discodermolide, a cytotoxic marine agent that stabilizes microtubules more potently than taxol, Biochemistry 35 (1996) 243–250.
[23] S.L. Mooberry, G. Tien, A.H. Hernandez, A. Plubrukarn, B.S. Davidson, Laulimalide and isolaulimalide, new paclitaxel-like microtubule-stabilizing agents, Cancer Res. 59 (1999) 653–660.
[24] A.E. Prota, K. Bargsten, D. Zurwerra, J.J. Field, J.F. Diaz, K.H. Altmann, et al., Molecular mechanism of action of microtubule-stabilizing anticancer agents, Science 339 (2013) 587–590.
[25] A.E. Prota, K. Bargsten, P.T. Northcote, M. Marsh, K.H. Altmann, J.H. Miller, et al., Structural basis of microtubule stabilization by laulimalide and peloruside A, Angew. Chem. Int. Ed. Eng. 53 (2014) 1621–1625.
[26] J.J. Field, B. Pera, E. Calvo, A. Canales, D. Zurwerra, C. Trigili, et al., Zampanolide, a potent new microtubule-stabilizing agent, covalently reacts with the taxane luminal site in tubulin alpha,beta-heterodimers and microtubules, Chem. Biol. 19 (2012) 686–698.
[27] B. Pera, M. Razzak, C. Trigili, O. Pineda, A. Canales, R.M. Buey, et al., Molecular recognition of peloruside A by microtubules. The C24 primary alcohol is essential for biological activity, Chembiochem 11 (2010) 1669–1678.
[28] A. Chan, P.M. Andreae, P.T. Northcote, J.H. Miller, Peloruside A inhibits microtubule dynamics in a breast cancer cell line MCF7, Investig. New Drugs 29 (2011) 615–626.
[29] K.A. Hood, L.M. West, B. Rouwe, P.T. Northcote, M.V. Berridge, S.J. Wakefield, et al., Peloruside A, a novel antimitotic agent with paclitaxel-like microtubule-stabilizing activity, Cancer Res. 62 (2002) 3356–3360.
[30] E. Hamel, B.W. Day, J.H. Miller, M.K. Jung, P.T. Northcote, A.K. Ghosh, et al., Synergistic effects of peloruside A and laulimalide with taxoid site drugs, but not with each other, on tubulin assembly, Mol. Pharmacol. 70 (2006) 1555–1564.

[31] A. Wilmes, K. Bargh, C. Kelly, P.T. Northcote, J.H. Miller, Peloruside A synergizes with other microtubule stabilizing agents in cultured cancer cell lines, Mol. Pharm. 4 (2007) 269–280.
[32] T.L. Hawkins, D. Sept, B. Mogessie, A. Straube, J.L. Ross, Mechanical properties of doubly stabilized microtubule filaments, Biophys. J. 104 (2013) 1517–1528.
[33] J. Lowe, H. Li, K.H. Downing, E. Nogales, Refined structure of alpha beta-tubulin at 3.5 A resolution, J. Mol. Biol. 313 (2001) 1045–1057.
[34] J.P. Snyder, J.H. Nettles, B. Cornett, K.H. Downing, E. Nogales, The binding conformation of Taxol in beta-tubulin: a model based on electron crystallographic density, Proc. Natl. Acad. Sci. U. S. A. 98 (2001) 5312–5316.
[35] S. Sharma, C. Lagisetti, B. Poliks, R.M. Coates, D.G. Kingston, S. Bane, Dissecting paclitaxel–microtubule association: quantitative assessment of the 2′-OH group, Biochemistry 52 (2013) 2328–2336.
[36] G.I. Georg, T.T. Chen, I. Ojima, D.M. Vyas., (Eds.) Edition 1, Chapter 15, 583, American Chemical Society, 1155 Sixteenth Street, NW, Washington, DC 20036, USA, 203–216.
[37] R. Matesanz, J. Rodriguez-Salarichs, B. Pera, A. Canales, J.M. Andreu, J. Jimenez-Barbero, et al., Modulation of microtubule interprotofilament interactions by modified taxanes, Biophys. J. 101 (2011) 2970–2980.
[38] E.M. Larsen, M.R. Wilson, J. Zajicek, R.E. Taylor, Conformational preferences of zampanolide and dactylolide, Org. Lett. 15 (2013) 5246–5249.
[39] R. Zhang, E. Nogales, A new protocol to accurately determine microtubule lattice seam location, J. Struct. Biol. 192 (2015) 245–254.
[40] M. Khrapunovich-Baine, V. Menon, C.P. Yang, P.T. Northcote, J.H. Miller, R.H. Angeletti, et al., Hallmarks of molecular action of microtubule stabilizing agents: effects of epothilone B, ixabepilone, peloruside A, and laulimalide on microtubule conformation, J. Biol. Chem. 286 (2011) 11,765–11,778.
[41] D.E. Pryor, A. O'Brate, G. Bilcer, J.F. Diaz, Y. Wang, Y. Wang, et al., The microtubule stabilizing agent laulimalide does not bind in the taxoid site, kills cells resistant to paclitaxel and epothilones, and may not require its epoxide moiety for activity, Biochemistry 41 (2002) 9109–9115.
[42] R.M. Buey, J.F. Diaz, J.M. Andreu, A. O'Brate, P. Giannakakou, K.C. Nicolaou, et al., Interaction of epothilone analogs with the paclitaxel binding site: relationship between binding affinity, microtubule stabilization, and cytotoxicity, Chem. Biol. 11 (2004) 225–236.
[43] M. Kikumoto, M. Kurachi, V. Tosa, H. Tashiro, Flexural rigidity of individual microtubules measured by a buckling force with optical traps, Biophys. J. 90 (2006) 1687–1696.
[44] A. Mitra, D. Sept, Taxol allosterically alters the dynamics of the tubulin dimer and increases the flexibility of microtubules, Biophys. J. 95 (2008) 3252–3258.
[45] E.A. Clark, P.M. Hills, B.S. Davidson, P.A. Wender, S.L. Mooberry, Laulimalide and synthetic laulimalide analogues are synergistic with paclitaxel and 2-methoxyestradiol, Mol. Pharm. 3 (2006) 457–467.
[46] A. Wilmes, D. O'Sullivan, A. Chan, C. Chandrahasen, I. Paterson, P.T. Northcote, et al., Synergistic interactions between peloruside A and other microtubule-stabilizing and destabilizing agents in cultured human ovarian carcinoma cells and murine T cells, Cancer Chemother. Pharmacol. 68 (2011) 117–126.
[47] D. Lyumkis, A.F. Brilot, D.L. Theobald, N. Grigorieff, Likelihood-based classification of cryo-EM images using FREALIGN, J. Struct. Biol. 183 (2013) 377–388.
[48] S.H. Scheres, RELION: implementation of a Bayesian approach to cryo-EM structure determination, J. Struct. Biol. 180 (2012) 519–530.
[49] F. DiMaio, Y. Song, X. Li, M.J. Brunner, C. Xu, V. Conticello, et al., Atomic-accuracy models from 4.5-A cryo-electron microscopy data with density-guided iterative local refinement, Nat. Methods 12 (2015) 361–365.
[50] A. Brown, F. Long, R.A. Nicholls, J. Toots, P. Emsley, G. Murshudov, Tools for macromolecular model building and refinement into electron cryo-microscopy reconstructions, Acta Crystallogr. D Biol. Crystallogr. 71 (2015) 136–153.
[51] R.M. Buey, I. Barasoain, E. Jackson, A. Meyer, P. Giannakakou, I. Paterson, et al., Microtubule interactions with chemically diverse stabilizing agents: thermodynamics of binding to the paclitaxel site predicts cytotoxicity, Chem. Biol. 12 (2005) 1269–1279.
[52] J.F. Diaz, R.M. Buey, Characterizing ligand-microtubule binding by competition methods, Methods Mol. Med. 137 (2007) 245–260.